Universität Leipzig

Fakultät für Mathematik und Informatik
Institut für Informatik

Evolution of Moisture Transport Patterns in the North Atlantic in different Climate scenarios

Masterarbeit

Leipzig, Mai 2024

vorgelegt von

Denis Streitmatter
Studiengang Master Informatik

Betreuende Hochschullehrer:
Dr. Baldwin Nsonga
Universität Leipzig, Abteilung für Bild und Signalverarbeitung
Prof. Dr. Gerik Scheuermann
Universität Leipzig, Abteilung für Bild und Signalverarbeitung

Abstract

The distribution and variability of precipitation in Europe are significantly influenced by moisture transport over the north(east)ern Atlantic. The objective of my master thesis is to analyze the evolution of moisture transport patterns in various future climate scenarios. The foundation of this research lies in the MPI-GE, the Max Planck Institute Grand Ensemble Dataset, comprising an ensemble of 100 members for different RCP (climate) scenarios up until 2100. Each member provides multiple fields of relevant climate data. A challenge will be the visualization of uncertainty stemming from 100 different simulations, which will not be straightforward.

To quantify moisture transport, an integrated water vapor transport (a combination of wind and specific moisture) scalar/vector field will be generated from the MPI-GE. Windowed Empirical Orthogonal Functions (EOFs) will be used to extract spatial-temporal patterns and simplify the data, making it easier to evaluate pattern evolution over time.

Contents

1   Introduction and Motivation

1.1   Motivation

Since the discovery (and further confirmation) of the greenhouse effect in the years from 1824 to 1900 [7, 8] humans came a long way of fighting the consequences of the increased greenhouse gas concentration in earth's atmosphere. In 1972 Sawyer summarized the knwoledge and predicted quite accurately the warming at the end of the century [25] Especially the last decades the climate crisis gained more and more attention, leading to the creation of multiple international organizations and institutions (e.g. the International Panel on Climate Change (IPCC) in 1988).

In 2019 more than 11,000 scientists from around the world released a declaration [22], calling governments from around the world to action. The mid and long-term consequences are manyfold and go far beyond the general rising of the worlds' average temperature (see Figure 1.1), e.g. shifts in circulation systems like the North Atlantic Oscillation (NAO) [32], which in turn also have varying consequences. Understanding what consequences may lay ahead of us is a crucial step in tackling these challanges, and this thesis aims to follow up on the research of Vietinghoff et al., trying to evaluate in a similar manner the systemic changes of moisture transport patterns in Europe and the northern Atlantic.

1.2   Climate and Climate Research

This section should give an introduction to the current state of climate research. Therefor it should explain what the current way of future climate predictions is (Coupled Models), how they work, and It should explain some part of the politics, who is involed in what and what the backroud of the most important projects (CMIP, ScenarioMIP …). It should be explained that the data used is the one that the highest council of fighting climate change uses for its report.

1.

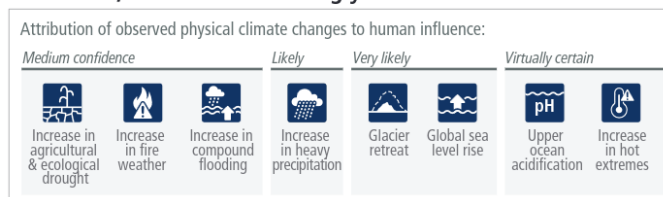**IPCC and the Coupled Model Intercomparison Project (CMIP)**
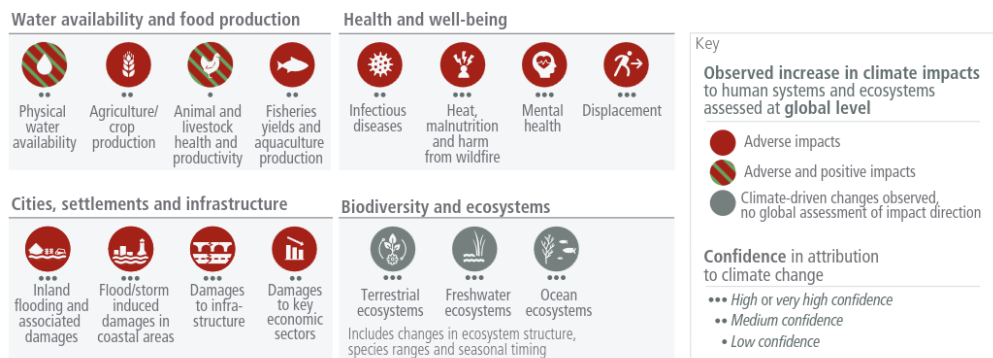
Figure 1.1: Impact of Climate Change for Humans, taken from [13]

The reason for the endorsement of the IPCC by the UN General Assembly 1988 was to prepare comprehensive reviews and report about the current state of scientific knowledge and research. Since then there were six assement cycles and six reports were published, condensing the research of the scientific community. Figure 1.1 is a graphic from the latest report for policy makers from 2023 [13], displaying the probable consequences for humans in climate change. A main source for such figures in the reports are so-called Global Coupled Models (GCM), trying to model the state and evolution of certain fields of earth data . They consist of multiple Models, each representing a major part of Earth's complex climate system (like atmosphere, hydrosphere, etc.), also allowing to model the dynamic interactions between these parts. In the mid 90s the Coupled Model Intercomparison Project (CMIP) was brought to life, with the aim of streamlining results of GCMs and making them compareable. CMIP provides the outer structure, amongst others what kind of simulations to produce (e.g. preindustrial control simulations, future scenarios etc.), what kinds of fields should be generated, what kind of resolutions to provide and also how these results should be serialized. Since then the results of CMIP played an increasingly major part in the reports of the IPCC [30], and are now even called "... one

of the foundational elements of climate science" [5]. CMIP is currently in its 6th phase, corresponding to the recently finished 6th Assessment Report of the IPCC [13].

The North Atlantic Oscillation

1.3 Research Questions and Thesis Structure

Structure:

1. **Preliminaries**: explain what climate simulations are, what cmip(6) is and its relation to the IPCC reports and what that means for the global fight against the climate crisis. This chapter should prepare the reader to understand all the related work in Chapter 4.

2. **Problem Analysis**: explain what I want to do using the CMIP6 simulations: Describe what the general plan is: Visualization of the moisture transport in Europe with the help. Also define what the goals of the visualizations are: Visualize different scenarios for comparison, visualize uncertainties of different members, visualize evolution over time, also try combining those. Here should be a graphic that explains the workflow that transforms a simulation into some nice pictures

3. **Related Work**: Show what efforts have already been done regarding analysis of moisture transport, future and past. Maybe preparing a comparison table would be good.

4. **Realization**: Describe in a step by step way what measures had been taken.

5. **Evaluation**: A little bit unsure how far I (as a CS person) can evaluate this, have to come up with a concept

6. **Conclusion**: Same as step before, but there will be something to write about after everything else is written

2 Basics

This section should explain the basic math to understand the aforementioned topics, not that much needed but still needs to be there.

2.1 (Uncertain) Fields

2.2 Empirical Orthogonal Functions

3 MPI GE CMIP6

The Max Planck Institute Grand Ensemble CMIP6 (MPI GE CMIP6) is a Single-model initial-condition large ensemble (in short: SMILE) [20]. This means that a single model was run with different initial condiditions but the same external forcings (e.g. greenhous gasses) mutiple times (⇒ ensemble). This makes it possible to seperate the internal variability from the responses to the external forcing, enabling researchers to better quantify the consequences of climate change (for example) . Additionally it makes the research of extreme weather phenomena (e.g. droughts, floods etc.) more robust in spite of their rare occurences [16]. As described in Section 1.2, Coupled models

The dataset chosen for this project is the *Max Planck Institute Grand Ensemble CMIP6* (from now on MPI-GE CMIP6), presented by Olonscheck et al. [20]. The reasons for choosing this dataset are manifold:

1. It uses the latest (6th) phase of the Coupled Model Intercomparison Project (CMIP6)

2. Compared to its predecessor (MPI-GE [17]) it provides high frequency output (6 hour intervals vs. monthly means), which enables taking short-lived weather events and structures (e.g. atmospheric rivers) into account which would be lost in the calculation of the mean

3.

This section should explain what datasets are available and why I chose the MPI-GE CMIP6 [20]

Maybe but the comparison table from [20] here and expand it a bit.

4   Related Work

This section outlies the current state-of-the-art in the main parts of this thesis explained in Section 1.3: Quantifying Moisture (Transport), extracting spatio-temporal patterns, tracking their change over time and visualizing the uncertain results in the end.

4.1 Motivation

As explained in Chapter 1, the approach of this thesis is motivated by the approach of Vietinghoff et al. in [32] and the affiliated dissertation [31], which tackles the issue of detecting critical points in unstable scalar fields. Hereby [32] analyzes the MPI GE [17] from the 5th phase of CMIP, an ensemble simulation with 50 members. The goal was to find the probable centers of pressure high/lows in the NAO pattern (see Section 1.2) and to track their shift over time. They employed a sliding window approach, computing the dominant pattern (see Section 2.2) for each window and member, and determine the likely areas of critical points by merging the results of different memebers per timestep. The centers of mass of these critical areas are then tracked over time to visualize the shift of the pressure high and low. The results show that the patterns do change, and this change is more pronounced if climate change is stronger. Also, there is no significant change if the climate remains stable.

4.2 Moisture Transport

To computationally extract any spatio-temporal patterns of moisture (transport), it first needs to be quantified in any way. The variable from the MPI GE CMIP6 used for this task is the *specific humidity*, which has no unit and is a float value between 0.0 and 1.0, denoting the percentage of water in the air at a specific gridpoint. The vast majority of literature regarding moisture transport use some form of vertically integrated humidity and the variants will be explained in the following section. A popular usage of these

quantifications was to find a filamentary weather structure called "Atmospheric Rivers"[1], a prominent way of water vapor transportation in the extratropic regions [9].

The most straightforward way of quantifying moisture is **Vertically Integrated Water Vapor (IWV)** [2, 9, 18, 26, 36], which is essentailly the vertical integral of the specific humidity q over the pressure levels p from earth's surface P_S to some upper limit in the atmosphere:

$$IWV = \frac{1}{g} \int_0^{P_s} q \ \mathrm{d}p \tag{4.1}$$

Similar to Equation 4.1, Zhu and Newell proposed in [38] **Vertical Integrated Moisture Transport (IVT)**, a way of moisture transport by vertically integrating over the different pressure levels the zonal (along latitude lines) and meridional (along longitude lines) fluxes. It became a popular metric for finding atmospheric rivers [9], sometimes alongside IWV [4]. IVT has the unit $\frac{kg}{ms}$ and is usually defined with

$$\overrightarrow{IVT} = \frac{1}{g} \int_0^{P_s} q \begin{pmatrix} u \\ v \end{pmatrix} \ \mathrm{d}p \tag{4.2}$$

or in a mathematically equivalent form [6]. Here u and v stand for the zonal and meridional components of the horizontal wind vector. While Equation 4.2 yields a vector field, the euclidian norm of said vector field

$$\|IVT\| = \frac{1}{g} \sqrt{(\int_0^{P_s} qu \ \mathrm{d}p)^2 + (\int_0^{P_s} qv \ \mathrm{d}p)^2} \tag{4.3}$$

is also a popular choice in detecting atmospheric rivers [21, 28] and other use cases [1].

The IVT is also part of the atmospheric moisture budget [34] (and similar in [27]) given by

$$\frac{1}{g} \frac{\delta}{\delta t} \int_0^{P_s} q \ \mathrm{d}p = -\nabla \cdot \frac{1}{g} \int_0^{P_s} q \begin{pmatrix} u \\ v \end{pmatrix} \mathrm{d}p + E - P$$

With E being the total evaporation and P the precipitation. Yang et al. showed in their report [34] the directions of moisture flux and its evolution in the last three decades. The analysis was done for all continental borders based on the big ERA5 reanalysis. The metrics used for this analysis were mostly the evaporation E, precipitation P and the moisture transport convergence $VIMC = \frac{1}{g} \int_0^{P_s} \nabla \cdot q \begin{pmatrix} u \\ v \end{pmatrix} \mathrm{d} p$ from Equation 4.2.

---

[1] earlier or alternative name: "Tropospheric Rivers"

Table 4.1: Overview table of patterns with moisture transport

Paper ID	Release Year	Pattern extraction	Area of Interest	Timescope	Time Resolution	Studied Season	Variable used for EOF
[29]	2020	SOMs	USA east	1979 to 2017	daily	all year	IVT norm
[1]	2022	EOF	China	1979 to 2010	daily	all year	IVT norm
[23]	1982	EOF	Northern hemishpere	1958 to 1973	monthly/yearly	all year	IWV, IVT_u IVT_v, combined
[6]	2003	EOF	mediterranian sea	1948 to 1996	6hr	DJF	P
[37]	2005	EOF	China	1951 to 1999	monthly	JJA	P
[10]	2018	EOF	USA (west coast)	1948 to 2017	daily	NDJF	IVT norm (assumed)
[12]	2014	EOF	western USA	1979 to 2010	6hr	DJF	IVT norm (assumed)
[40]	2018	EOF	TEIOWP	1961 to 2015	monthly	JJA	IVT
[39]	2020	EOF	TEIOWP	1958 to 2018	6hr/monthly	JJA	Integrated Water Vapor Sink
[35]	2013	EOF	East Asia	1997 to 2002		JJA	IVT_u IVT_v
[14]	2012	EOF	East Asia	1979 to 2009	monthly	summer	IVT

While the integration in the previous equations integrates from the surface to the outer border of the atmosphere (0 Pa), it is quite common to integrate up until the limit of 300 hPa [1, 10, 12, 38], since the amount of moisture in the regions from 300 hPa to 0 Pa is quite neglible and amounts in total to about 2-3 cm/year in terms of freshwater flux [37].

There are also some other notable other algorithms, namely stable oxygen isotope investigation [15] and langragian backwards trajectories [36], but both rather look for the origin of the water vapor instead of its destination and are therefor out of scope for this thesis.

4.3 Pattern analysis regarding IVT

While there are many areas of interest for the application of EOF, this Section will give an overview what kind of pattern analysis has been performed in relation with IVT data. An overview of datasets, timescopes and other metadata is given in Table 4.1.

Although most found related work uses EOF analysis, Teale and Robinson employ an approach using Self Organizing Maps (SOMs) to detect patterns of moisture transport in the eastern United States. SOMs are a machine learning approach to reduce data dimensionality, producing a 2D map of higher dimensional data. While they acknowledge the [CITE?] efficiency of EOF to extract dominant patterns, they emphasize the problem of required orthogonality of modes, which is not given for SOMs. The results show that fluxes with the highest moisture content occur less frequently than those with less moisture. But despite the higher moisture content, fluxes with lower moisture transport dominate water vapor movement due to their prevalence. Many of these fluxes meet typical criteria for atmospheric rivers, with varying trajectories and sources suggesting diverse mechanisms of formation. The temporal variability in monthly flux frequencies correlates with regional precipitation patterns, indicating that this approach is a valuable framework for studying precipitation changes [29].

Ayantobo et al. analysed the primary six modes of EOF in China, which was grouped in deifferent regions for comparison. While the variances of IVT in eastern to southern China were quite high, the variances in northern China were quite low. It was shown by comparing the temporal patterns of the primary mode of EOF with the ENSO, that these patterns were related. The cross-wavelet coherence revealed that IVT and ENSO time-series were coherent, which implies that increased IVT was prevalent linked to increased ENSO activities [1].

Published in 1982, Salstein et al. provided the first example of calculating EOF on IVT. Based on data from 91 weather stations, they computed the IVT of the whole northern hemisphere. Statistical siginificance was determined by employing a Monte Carlo testing method. EOF was computed on the IWV, the zonal and meridional IVT fields respectively, but they also evaluated an approach of combining both IVT components in one data vector. They reported the significance of the primary mode of IWV, encoding nearly half (44 %) of variance of the data.

Fernández et al. analyzed the precipitation modes in the mediterranean sea and linking them to the moisture transport in the same area. A goal of this analysis was to contribute to the understanding of the reduction of precipitation which happened in the area as well as to the low-frequency precipitation variability, leading to multiyear drought periods. They employed multiple methods of validating their data: The precipitation data as well as the wind/moisture data for IVT were validated with data from actual weather stations. The stability of the eigenvectors was tested with a Monte Carlo simulation, comparing the variability of actual data with random test data, while degeneracy of the EOF modes was tested using the method of North et al. [19]. Results of the analysis identify the interpretation of the three main precipitation modes: The first mode (22 % variance) seems to be linked to the NAO and Atlantic Storm tracks and associated moisture transports, while the second mode (16 %) represents the internal redistribution of moisture in the mediterranean basin between the estern and western parts. The third mode (11 %) explains increased precipitation in the northern part of the domain. Additionally, moisture transport during positive and negative phases of leading mode showed increased inflow of moisture from the west [6].

Similar to [6], Zhou and Yu analyzed the anoumalous summer rainfall patterns over China and link them to water vapor transport. They confirmed their results by using a second dataset for IVT calculation. They showed that the primary mode of anomalous rainfall is associated with heavier rainfall in the Yangtze river region, while the same applies to the second mode and the Huaihe river. Connecting these patterns to moisture transport, they identified the different ways how these heavier rain areas are coming about by

cerain convergences of water vapor transports. Furthermore they compared the supply of anoumalous rainfall patterns to the one of normal monsoon rainfall, revealing that those differ significantly [37].

In [10], the authors calculate rotated EOF on IVT data and try to analyze the relation between the 15 most dominant modes and the occurence of atmospheric rivers (AR) on the USA west coast. For this they divided the coast into different regions and linked the activity (positive and negative) of the corresponding temporal pattern of each mode to the occurence of atmospheric rivers. It was found that a few modes seem very influational for certain reagions' AR activity, while others seem to play no role at all. They also identfied favorable and unfavorable circulation states (e.g. amongst others a low pressure anomaly in a certain region) for AR occurce [10].

Kim and Alexander showed in their analysis the connection of the IVT patterns in the western USA to three different ENSO events (eastern pacific El Niño (EPEN), central pacific El Niño (CPEN) and La Niña (NINA)). While EPEN events are associated with large positive IVT anomalies from the subtropical Pacific to the north-western USA, CPEN events lead to enhanced moisture transport to the southern USA. During NINA events the mean IVT anomaly is flipped in comparison to EPEN and CPEN. Furthermore it was shown that IVT patterns computed for these events differ significantly from the ones computed for neutral years. Furthermore the results were connected to precipitation anomalies on the USA west coast, showing huge differences (especially for the northern part of the coast) for EPEN and CPEN events. But the authors also emphasize that while the suggestions are strong, exceptions occur (e.g. one El Niño leading to a dry winter, another to the opposite) and need to be studied in greater detail.

Similar to [32] and the approach of this thesis, Zou et al. applied a sliding window approach to IVT patterns in the tropical Indian Ocean–western Pacific to analyze the evolution over time. For the studied period from 1961 to 2015, they studied every 20 year period with a 5 year sliding window, computing Multivariate EOFs for each window, resulting in vector fields of patterns. The results show that the two most significant modes show significant changes in the mid 80s: The primary mode is characterized by a anti-cyclonic pattern in the north-western Pacific, which shifts significantly to the south. An analysis of the relation to sea surface temperature (SST) revealed that the correlation between the mode and SST rose in the mid 80s, from weakly correlated to significant positive correlation between IVT and SST anomalies. Furthermore, the primary mode seems to be regulated significantly bei ENSO. The second most significant mode is related to the variablility of the tropical Indian Ocean dipole (defined by the differences in average SST) [40].

A different approach was employed by [39], evaluating the EOF patterns of vertically integrated apparent moisture sink. Results indicate that the primary mode is a southwest-northeast oriented dipole, while the secondary mode is a southwest-northeast oriented tripole. The primary mode seems to be heavily regulated by the ENSO in the previous winter season, while the second mode seems to originates from internal atmospheric variability. Based on the much higher standard deviations in ENSO years, it seems that water vapor source and sink tend to be dominated by the primary mode in ENSO years, while the secondary mode is prevalent in non-ENSO years.

While the main focus of [35] is to evaluate and compare a regional air-sea coupled model, they also performed EOF analysis on the zonal and meridional components of IVT, respectively. They used the results to evaluate the connection to SST, revealing that the results from the regional coupled model aligns better with results from other datasets and reality than the regional uncoupled model.

Li and Zhou evaluated the connection of the IVT-EOF patterns to ENSO in the asian western northern Pacific. They used a different approach then most in applying EOF to IVT, by concatenating the meridional and zonal components in one matrix and calculating EOF on it. To confirm their results, they compared the results with another reanalysis from the same (and a larger) region. Furthermore, these IVT patterns were linked to the SST. They revealed the characteristics of the two most significant modes, but most prominently they showed the quasi-4-year coupling of the two most prominent modes with ENSO [14].

4.4 Uncertainty Visualisation

Since the used dataset (see Chapter 3) is an ensemble simulation consisting of 50 members, most of the figures and other visual representations in this thesis need to display the uncertainty stemming from them. This section summarizes advances fitting for this topic, giving a frame of references of current possibilities of vizualizing uncertainty.

Kamal et al. give a recent overview over the whole topic of uncertainty visualization: From the introduction to the whole concept of uncertainty, to the differentiation between different kinds of uncertainty in the visualisation process. They grouped all kinds of representing uncertainty in two categories: quatification, consisting of mostly mathematical approaches of handling uncertain data, and visualisation, displaying the uncertain data in a way directly. An overview of the different kinds of uncertainty visualization were given: Manipulation of attributes (like shading), animation, visual variables (like color, hue, brightness), graphical techniques like box/scatter plots and glyphs. Furthermore, recent advances in uncertainty visualization are given, with a special emphasis on ensemble

(simulation) data, big data and machine learning, listing the most prominent areas where the presentation of uncertainity is crucial. In the end, a framework for evaluating uncertainity visualization is presented, followed by an overview of possible future research directions [11].

A way of using animation to display uncertainty in scalar fields was shown by Coninx et al. Their goal was to enrich the usual display of scalar fields with colormaps with additional uncertainity information. The tool of choice here was animated Perlin noise, and the uncertainity was presented by modifying the noise mask with the uncertainity information at each point. The results were tested using a psychophysical evaluation of contrast sensitivity thresholds [3], evaluating effective parameters for proper presentation of the uncertain area [3].

Sanyal et al. proposed Noodles, a tool for displaying uncertainty in weather ensemble simulations. It employs three different ways of displaying uncertain isocontours: ribbon, glyphs and spaghetti plots. Additionally, they added tools for exploring the uncertainty of datasets, like an colormap of the whole dataset uncertainty. Uncertainty in spaghetti plots is clear (one line per member), but gets confusing and chaotic quickly. The glyphs display the uncertainity by different sizes, and can be displayed on the whole map or alogside means of isocontours. Ribbons condense the information of multiple lines by adapting the ribbon width to the uncertainty of isolines at a specific gridpoint. The resulting tool was tested by two meteorologists, and classified the results as beneficial [24].

Another way of visualizing groups of isocontours are contour boxplots proposed in [33], grouping isocontours together in a similar way like conventional boxplots. This means that the easiest default presentation (spaghetti plots) is replaced by popular boxplot stats: The median, the mean, the quartiles around that mean, the whole range and the outliers (not part of the whole range). But the implementation is not as straight forward as in conventional boxplots. To quantify the aforementioned statistics, Whitaker et al. propose a data depth based approach, which encodes how much a particular sample is centrally located in its function (or in this case: How central is a isocontour to a whole set of isocontours). While the results look very promising, it lacks a publicly available implementation, making it hard to use the approach.

5 METHODOLOGY

5.1 OVERVIEW

Explain what I want to do using the CMIP6 simulations: Describe what the general plan is: Visualisation of the moisture transport in Europe with the help . Also define what the goals of the visualisations are: Visualize different scenarios for comparison, visualize uncertainties of different members, visualize evolution over time, also try combining those. Here should be a graphic that explains the workflow that transforms a simulation into some nice pictures

5.2 PREPROCESSING

The goal of this step is to generate an IVT field (see Chapter 4) from the MPI GE CMIP6 (see Chapter 3). The steps to complete this task are quite straight forward:

1. Load four different fields for each time period in each member in each szenario: Specific humidity *hus*, eastward horizontal wind *ua*, northward horizontal wind *va* and surface pressure *ps*. Here the geographical box around the area of interest is cut out: Europe and the North Atlantic (Longitude: $-90 \rightarrow 40$, Latitude: $20 \rightarrow 80$, based on [32])

2. For each geographical gridpoint (*lon*, *lat*) and timestep: Calculate the integrals of hte product of wind components and specific humidity over the vertical pressure levels $\frac{1}{g} \int_{p_S}^{0} hus * ua$ and $\frac{1}{g} \int_{p_S}^{0} hus * va$, with g being the gravitational acceleration ($9.806 \frac{m}{s}$)

3. Save the results for each time period in each member in each szenario in a NetCDF file for the further steps.

The calculations were performed on the high performance computing cluster[1] of the German Climate Calculations Center (DKRZ), due to the MPI GE CMIP6 is saved there and downloading the data would take a lot of time. This also result in the goal of this step

---

[1]https://docs.dkrz.de/doc/levante/

to minimize the hours on the HPC system since they get billed by the time using nodes. Although these steps seem easy, due to the large sizes of the datasets and other issues many challenges were met. In the following those will be explained with regard to the step they ocurred in.

1. **Data Loading**

   - cutting out geobox

   - slow IO → started using dask+xarray

2. **Vertical integration**

   - calculate hybrid sigma pressure levels for each gridpoint and timestep to get the x values for integration

   - describe my idea of testing the integration

6 RESULTS

7 Conclusions and Future Work

7.1 Conclusions

7.2 Future Work

Acronyms

PCA   Principal component analysis

SNF   Smith normal form

TDA   Topological data analysis

Glossary

LaTeX A document preparation system

$\mathbb{R}$ The set of real numbers

Bibliography

1. O. O. Ayantobo, J. Wei, B. Kang, and G. Wang. "Integrated moisture transport variability over China: patterns, impacts, and relationship with El Nino–Southern Oscillation (ENSO)". en. *Theoretical and Applied Climatology* 147:3-4, 2022, pp. 985–1002. ISSN: 0177-798X, 1434-4483. DOI: 10.1007/s00704-021-03864-x.

2. J.-W. Bao, S. A. Michelson, P. J. Neiman, F. M. Ralph, and J. M. Wilczak. "Interpretation of Enhanced Integrated Water Vapor Bands Associated with Extratropical Cyclones: Their Formation and Connection to Tropical Moisture". en. *Monthly Weather Review* 134:4, 2006, pp. 1063–1080. ISSN: 1520-0493, 0027-0644. DOI: 10.1175/MWR3123.1.

3. A. Coninx, G.-P. Bonneau, J. Droulez, and G. Thibault. "Visualization of uncertain scalar data fields using color scales and perceptually adapted noise". en. In: *Proceedings of the ACM SIGGRAPH Symposium on Applied Perception in Graphics and Visualization.* ACM, Toulouse France, 2011, pp. 59–66. ISBN: 978-1-4503-0889-2. DOI: 10.1145/2077451.2077462.

4. J. Eiras-Barca, S. Brands, and G. Miguez-Macho. "Seasonal variations in North Atlantic atmospheric river activity and associations with anomalous precipitation over the Iberian Atlantic Margin". en. *Journal of Geophysical Research: Atmospheres* 121:2, 2016. _eprint: https://onlinelibrary.wiley.com/doi/pdf/10.1002/2015JD023379, pp. 931–948. ISSN: 2169-8996. DOI: 10.1002/2015JD023379.

5. V. Eyring, S. Bony, G. A. Meehl, C. A. Senior, B. Stevens, R. J. Stouffer, and K. E. Taylor. "Overview of the Coupled Model Intercomparison Project Phase 6 (CMIP6) experimental design and organization". en. *Geoscientific Model Development* 9:5, 2016, pp. 1937–1958. ISSN: 1991-9603. DOI: 10.5194/gmd-9-1937-2016.

6. J. Fernández, J. Sáenz, and E. Zorita. "Analysis of wintertime atmospheric moisture transport and its variability over southern Europe in the NCEP Reanalyses". en. *Climate Research* 23, 2003, pp. 195–215. ISSN: 0936-577X, 1616-1572. DOI: 10.3354/cr023195.

7. E. Foote. "Circumstances affecting the heat of the sun's rays". *Am. J. Sci. Arts* 22:66, 1856, pp. 383–384.

Bibliography

8. J. Fourier. "Remarques générales sur les températures du globe terrestre et des espaces planétaires". In: *Annales de Chemie et de Physique*. Vol. 27. 1824, pp. 136–167.

9. L. Gimeno, R. Nieto, M. Vázquez, and D. Lavers. "Atmospheric rivers: a mini-review". *Frontiers in Earth Science* 2, 2014. ISSN: 2296-6463.

10. K. Guirguis, A. Gershunov, R. E. S. Clemesha, T. Shulgina, A. C. Subramanian, and F. M. Ralph. "Circulation Drivers of Atmospheric Rivers at the North American West Coast". en. *Geophysical Research Letters* 45:22, 2018. _eprint: https://onlinelibrary.wiley.com/doi/pdf/10.1029/2018GL079249, pp. 12, 576–12, 584. ISSN: 1944-8007. DOI: 10.1029/2018GL079249.

11. A. Kamal, P. Dhakal, A. Y. Javaid, V. K. Devabhaktuni, D. Kaur, J. Zaientz, and R. Marinier. "Recent advances and challenges in uncertainty visualization: a survey". en. *Journal of Visualization* 24:5, 2021, pp. 861–890. ISSN: 1343-8875, 1875-8975. DOI: 10.1007/s12650-021-00755-1.

12. H.-M. Kim and M. A. Alexander. "ENSO's Modulation of Water Vapor Transport over the Pacific–North American Region". en. *Journal of Climate* 28:9, 2015, pp. 3846–3856. ISSN: 0894-8755, 1520-0442. DOI: 10.1175/JCLI-D-14-00725.1.

13. H. Lee, K. Calvin, D. Dasgupta, G. Krinner, A. Mukherji, P. Thorne, C. Trisos, J. Romero, P. Aldunce, and A. C. Ruane. "Climate change 2023 synthesis report summary for policymakers". *CLIMATE CHANGE 2023 Synthesis Report: Summary for Policymakers*, 2024.

14. X. Li and W. Zhou. "Quasi-4-Yr Coupling between El Niño–Southern Oscillation and Water Vapor Transport over East Asia–WNP". en. *Journal of Climate* 25:17, 2012, pp. 5879–5891. ISSN: 0894-8755, 1520-0442. DOI: 10.1175/JCLI-D-11-00433.1.

15. Y. Ma, M. Lu, H. Chen, M. Pan, and Y. Hong. "Atmospheric moisture transport versus precipitation across the Tibetan Plateau: a mini-review and current challenges". en.

16. N. Maher, S. Milinski, and R. Ludwig. "Large ensemble climate model simulations: introduction, overview, and future prospects for utilising multiple types of large ensemble". en. *Earth System Dynamics* 12:2, 2021, pp. 401–418. ISSN: 2190-4987. DOI: 10.5194/esd-12-401-2021.

17. N. Maher, S. Milinski, L. Suarez-Gutierrez, M. Botzet, M. Dobrynin, L. Kornblueh, J. Kröger, Y. Takano, R. Ghosh, C. Hedemann, C. Li, H. Li, E. Manzini, D. Notz, D. Putrasahan, L. Boysen, M. Claussen, T. Ilyina, D. Olonscheck, T. Raddatz, B. Stevens, and J. Marotzke. "The Max Planck Institute Grand Ensemble: Enabling the Exploration of

Climate System Variability". en. *Journal of Advances in Modeling Earth Systems* 11:7, 2019, pp. 2050–2069. ISSN: 1942-2466, 1942-2466. DOI: 10.1029/2019MS001639.

18. P. J. Neiman, F. M. Ralph, G. A. Wick, J. D. Lundquist, and M. D. Dettinger. "Meteorological Characteristics and Overland Precipitation Impacts of Atmospheric Rivers Affecting the West Coast of North America Based on Eight Years of SSM/I Satellite Observations". en. *Journal of Hydrometeorology* 9:1, 2008, pp. 22–47. ISSN: 1525-7541, 1525-755X. DOI: 10.1175/2007JHM855.1.

19. G. R. North, T. L. Bell, R. F. Cahalan, and F. J. Moeng. "Sampling Errors in the Estimation of Empirical Orthogonal Functions". EN. *Monthly Weather Review* 110:7, 1982. Publisher: American Meteorological Society Section: Monthly Weather Review, pp. 699–706. ISSN: 1520-0493, 0027-0644. DOI: 10.1175/1520-0493(1982)110<0699:SEITEO>2.0.CO;2.

20. D. Olonscheck, L. Suarez-Gutierrez, S. Milinski, G. Beobide-Arsuaga, J. Baehr, F. Fröb, L. Hellmich, T. Ilyina, C. Kadow, D. Krieger, H. Li, J. Marotzke, É. Plésiat, M. Schupfner, F. Wachsmann, K.-H. Wieners, and S. Brune. *The new Max Planck Institute Grand Ensemble with CMIP6 forcing and high-frequency model output.* en. preprint. Preprints, 2023. DOI: 10.22541/essoar.168319746.64037439/v1.

21. A. M. Ramos, R. Nieto, R. Tomé, L. Gimeno, R. M. Trigo, M. L. R. Liberato, and D. A. Lavers. "Atmospheric rivers moisture sources from a Lagrangian perspective". en. *Earth System Dynamics* 7:2, 2016, pp. 371–384. ISSN: 2190-4987. DOI: 10.5194/esd-7-371-2016.

22. W. J. Ripple, C. Wolf, T. M. Newsome, P. Barnard, and W. R. Moomaw. "World Scientists' Warning of a Climate Emergency". en. *BioScience*, 2019, biz088. ISSN: 0006-3568, 1525-3244. DOI: 10.1093/biosci/biz088.

23. D. A. Salstein, R. D. Rosen, and J. P. Peixoto. "Modes of Variability in Annual Hemispheric Water Vapor and Transport Fields". en. *Journal of the Atmospheric Sciences* 40:3, 1983, pp. 788–804. ISSN: 0022-4928, 1520-0469. DOI: 10.1175/1520-0469(1983)040<0788:MOVIAH>2.0.CO;2.

24. J. Sanyal, Song Zhang, J. Dyer, A. Mercer, P. Amburn, and R. J. Moorhead. "Noodles: A Tool for Visualization of Numerical Weather Model Ensemble Uncertainty". en. *IEEE Transactions on Visualization and Computer Graphics* 16:6, 2010, pp. 1421–1430. ISSN: 1077-2626. DOI: 10.1109/TVCG.2010.181.

25. J. S. Sawyer. "Man-made carbon dioxide and the "greenhouse" effect". *Nature* 239:5366, 1972, pp. 23–26.

26. P. Schluessel and W. J. Emery. "Atmospheric water vapour over oceans from SSM/I measurements". en. *International Journal of Remote Sensing* 11:5, 1990, pp. 753–766. ISSN: 0143-1161, 1366-5901. DOI: 10.1080/01431169008955055.

27. R. Seager, H. Liu, Y. Kushnir, T. J. Osborn, I. R. Simpson, C. R. Kelley, and J. Nakamura. "Mechanisms of Winter Precipitation Variability in the European–Mediterranean Region Associated with the North Atlantic Oscillation". en. *Journal of Climate* 33:16, 2020, pp. 7179–7196. ISSN: 0894-8755, 1520-0442. DOI: 10.1175/JCLI-D-20-0011.1.

28. P. M. Sousa, A. M. Ramos, C. C. Raible, M. Messmer, R. Tomé, J. G. Pinto, and R. M. Trigo. "North Atlantic Integrated Water Vapor Transport—From 850 to 2100 CE: Impacts on Western European Rainfall". en. *Journal of Climate* 33:1, 2020, pp. 263–279. ISSN: 0894-8755, 1520-0442. DOI: 10.1175/JCLI-D-19-0348.1.

29. N. Teale and D. A. Robinson. "Patterns of Water Vapor Transport in the Eastern United States". *Journal of Hydrometeorology* 21:9, 2020, pp. 2123–2138. ISSN: 1525-755X, 1525-7541. DOI: 10.1175/JHM-D-19-0267.1.

30. L. Touzé-Peiffer, A. Barberousse, and H. Le Treut. "The Coupled Model Intercomparison Project: History, uses, and structural effects on climate research". en. *WIREs Climate Change* 11:4, 2020, e648. ISSN: 1757-7780, 1757-7799. DOI: 10.1002/wcc.648.

31. D. Vietinghoff. "Critical Points of Uncertain Scalar Fields", 2024.

32. D. Vietinghoff, C. Heine, M. Bottinger, N. Maher, J. Jungclaus, and G. Scheuermann. "Visual Analysis of Spatio-Temporal Trends in Time-Dependent Ensemble Data Sets on the Example of the North Atlantic Oscillation". en. In: *2021 IEEE 14th Pacific Visualization Symposium (PacificVis)*. IEEE, Tianjin, China, 2021, pp. 71–80. ISBN: 978-1-66543-931-2. DOI: 10.1109/PacificVis52677.2021.00017.

33. R. T. Whitaker, M. Mirzargar, and R. M. Kirby. "Contour Boxplots: A Method for Characterizing Uncertainty in Feature Sets from Simulation Ensembles". *IEEE Transactions on Visualization and Computer Graphics* 19:12, 2013, pp. 2713–2722. ISSN: 1077-2626. DOI: 10.1109/TVCG.2013.143.

34. Y. Yang, C. Liu, N. Ou, X. Liao, N. Cao, N. Chen, L. Jin, R. Zheng, K. Yang, and Q. Su. "Moisture Transport and Contribution to the Continental Precipitation". en. *Atmosphere* 13:10, 2022, p. 1694. ISSN: 2073-4433. DOI: 10.3390/atmos13101694.

35. S. Yao, Q. Huang, Y. Zhang, and X. Zhou. "The simulation of water vapor transport in East Asia using a regional air–sea coupled model". en. *Journal of Geophysical Research: Atmospheres* 118:4, 2013, pp. 1585–1600. ISSN: 2169-897X, 2169-8996. DOI: 10.1002/jgrd.50089.

36. N. Zhao, A. Manda, X. Guo, K. Kikuchi, T. Nasuno, M. Nakano, Y. Zhang, and B. Wang. "A Lagrangian View of Moisture Transport Related to the Heavy Rainfall of July 2020 in Japan: Importance of the Moistening Over the Subtropical Regions". en. *Geophysical Research Letters* 48:5, 2021, e2020GL091441. ISSN: 0094-8276, 1944-8007. DOI: 10.1029/2020GL091441.

37. T.-J. Zhou and R.-C. Yu. "Atmospheric water vapor transport associated with typical anomalous summer rainfall patterns in China". en. *Journal of Geophysical Research: Atmospheres* 110:D8, 2005, 2004JD005413. ISSN: 0148-0227. DOI: 10.1029/2004JD005413.

38. Y. Zhu and R. E. Newell. "A Proposed Algorithm for Moisture Fluxes from Atmospheric Rivers". en. *Monthly Weather Review* 126:3, 1998, pp. 725–735. ISSN: 0027-0644, 1520-0493. DOI: 10.1175/1520-0493(1998)126<0725:APAFMF>2.0.CO;2.

39. M. Zou, S. Qiao, L. Chao, D. Chen, C. Hu, Q. Li, and G. Feng. "Investigating the Interannual Variability of the Boreal Summer Water Vapor Source and Sink over the Tropical Eastern Indian Ocean-Western Pacific". en. *Atmosphere* 11:7, 2020, p. 758. ISSN: 2073-4433. DOI: 10.3390/atmos11070758.

40. M. Zou, S. Qiao, T. Feng, Y. Wu, and G. Feng. "The inter-decadal change in anomalous summertime water vapour transport modes over the tropical Indian Ocean–western Pacific in the mid-1980s". en. *International Journal of Climatology* 38:6, 2018, pp. 2672–2685. ISSN: 0899-8418, 1097-0088. DOI: 10.1002/joc.5452.